J. Appl. Comput. Mech., 9(1) (2023) 95-112
DOI: 10.22055/jacm.2022.40364.3567

ISSN: 2383-4536
jacm.scu.ac.ir

Shahid Chamran University of Ahvaz

Journal of Applied and Computational Mechanics

Research Paper

CFD Analyses and Comparison of the Effect of Industrial Heat Sinks in Subsea Control System (SCS)

Jafar Mahmoudi

KTH, School of Industrial Engineering and Management, Department of Sustainable Production Development, Stockholm, Sweden

Received March 25 2022; Revised May 23 2022; Accepted for publication July 04 2022.
Corresponding author: J. Mahmoudi (Mahmoudi@kth.se)

Abstract. This article is part of the e-cooling project which has been granted by OutoKumpu and Intel. The author has been project manager aiming for optimization of the heat sink application. In this regard, several articles through 2006 to 2012, have been published to explain the chain of the process (casting, machining, welding) using the Pin-Fin technology. In 2011 to 2015, The project has been recapped and aiming to develop next design heatsink (combined copper- Aluminum heat sink) with special focus for the subsea application. The Risk analyses of the new heat sink design have also been studied. A new model has been developed for industrial production/ optimization process from casting to final processing. The mathematical modeling has been primarily employed to solve the source code addressing the energy of the dissipation rate using the 3D Navier-Stokes equations. The Ansys Fluent has been employed as the modeling software to implement the source term as subroutine. In this industrial research work the implementation of the mathematical modeling in the Ansys Fluent software is a critical part of the work aiming for design and optimization of the heat sink within SCI application.

Keywords: Electronic reliability, Heat sink design, Plate fin heat sinks, Conjugate heat transfer, Subsea control system (SCS).

1. Introduction

The Central Processing Unit (CPU) of a computer must continuously be cooled to maintain its temperature within the manufacture's specifications. It can be cooled using an attached heat sink with the heat dissipated to the air that is supplied by a fan or flow naturally. There are two main methods to provide the air known as the active and passive techniques [1]. In the active approach, a small fan is directly mounted on the heat sink, while the passive one has a fan which is installed in the rear wall of the case. The active heat sink solution is not a cost-effective design due to the server cost constraints placed on the desktop computers. Also, a limitation of the case fan is that most of its delivered air bypasses the heat sink [2]. If the airflow rate (or velocity) that passes over the sink is small, it will require a large heat sink increasing the manufacturing cost, which is an important parameter in design of heat sinks [3]. Hence, it is essential to circulate the airflow properly to achieve a relatively high heat transfer coefficient, which can be provided by heat sinks.

Typically, heat sinks have some fins that are utilized to enhance the heat transfer [4] and ensure the electronic device reliability [5, 6] with ever-increasing power dissipation and circuit density [7, 8]. There are three main types of heat sinks, namely, the plate-fin, pin-fin, and the micro-channel one [9]. The plate-fin type has the benefits of a slight drop in pressure, simple design and fast manufacturing. On the other hand, the pin-fin heat sink has the benefits of a high heat transfer rate and even thermal efficiency irrespective of the fluid flow direction [10-11]. Note that these two types are also presented with various configurations in their shape, geometry and orientation, such as the wavy or splayed heat sink [12-13] in the literature. In addition, the strengths of the plate-fin and pin-fin heat sinks have been merged in a format known as Plate-Pin Fin Heat Sinks (PPFHS) [14-16]. Also, the micro-channel type has small surface area and its compactness provides the benefit of using low amount of material and reducing the size [17]. This type of heat sink is also available in another scale presented as the mini-channel type [18].

Previous efforts to analyze the three-dimensional computational modeling of the referred heat sinks can be found in many publications, such as the recently published works in references [18-30]. Among them, Zhou et al. [31] tried to improve the performance of PPFHSs by implementing a finite volume-based simulation in CFD software. They concluded that all PPFHS will not necessarily lead to a better overall performance than the plate fin heat sink. Al-Damook [32] carried out experimental and numerical analyses on pin fin heat sinks with multiple perforations and reported the enhancement of heat transfer. Ong et al. [24] evaluate cooling performance of plate-fin heat sinks for one and two-dimensional heat flows. In their CFD simulation, the effect of aspect ratio is emphasized which is defined as the ratio of heat source the surface area over the heat. Meng et al. [21] investigated the effect of cutting the corner portion of a straight fin heat sink which was considered the stagnation area of heat transfer. They conclude that it leads to the reduction of thermal resistance and improvement of the heat transfer coefficients. Studies on different improvised fins of heat sinks such as the strip-fin and the louvered fins are performed as well in [33-35]. Despite these valuable efforts, the area is still open to having heat sinks with new designs and better performance.

Published online: July 14 2022

Reliability is a key criterion in measuring the performance of technical systems such as SCS. To provide a proper reliability analysis followed by the fulfillment of safety requirements in SCS, it is essential to identify mechanisms and modes of failure in components as well as to calculate the values of failure rate.

Failure of any component in SCS may cause a huge loss in several aspects of the system, such as production. Also, it results in a substantial increase in the environment's safety risks. For instance, consider the Subsea Control Module (SCM), which is a main part of a typical industry-based heat sink referred by production loss in a subsea system.

Another important issue is the optimization of heat sinks, which is addressed in works such as [9, 36-39]. Al-Damook et al. [36] investigated the design and optimization of single rectangular notch perforation in pin fin heat sinks. They reported increased heat transfer and reduced fan power as a result of using the perforations. Ahmed et al. [37] reviewed the optimization of various heat sinks with more concentration on the micro-channel types. Khattaf and Muhammad Ali [4] have recently investigated the different optimization strategies considering the flow type and specimen geometry. Lindstedt et al. [39] presented some expressions for the optimal dimensions of rectangular, triangular, and trapezoidal fins. They also investigated the minimization of the mass of a plate fin heat sink at a constant fan power by optimizing the geometrical variables and component locations on the base plate. Also, topology optimization is a new technique capable of optimizing the configuration of heat sinks without requiring a specified shape of the fin, which is addressed in [9]. Also, note that while the optimization is commonly known to be useful, its computational burden has prevented some researchers to include it in their analyses. In this work, it is considered though.

Despite the valuable efforts made by the researchers of the area, the challenge to disperse the generated heat properly and keep a balanced temperature of the CPU, and reduce the volume, cost, and weight of the heat sinks is an open topic. Innovate designs and models are highly demanded [4] to direct sufficient airflow to the CPU heat sink leading to higher values of heat transfer coefficient and proper heat dissipation. This paper addresses this issue and tries to propose a procedure to improve the effectiveness of heat sinks made of aluminum and copper metals. In this regard, initially, the proposed model is explained including its theoretical formulations and simulations process. Then, the model is validated for aluminum heat sinks followed by its usage for two cases of copper heat sinks. The first case is the rectangular heat sink based on the straight fins and the second one is an automotive-based heat sink without louver. Finally, the optimization of the model is discussed for another two cases by changing the values of some parameters.

2. The Proposed Model

In this section, the developed model is explained in two steps. Firstly, the theoretical procedure is described and then the simulation of the model in a CFD software is defined.

2.1. Theoretical approach

The theoretical background of this work is based on the previous research of the author in reference [40] including the explanations of the basic features. Herein, the numerical simulation is used to gain some insight into heat sink's integrated convection-conduction heat transfer. For this purpose, a set of three dimensional Navier-Stokes equations is adopted as a mathematical model of the mechanism for conservation of momentum. Also, this is based on the assumption of continuum.

Moreover, the theory of k-ε turbulence is used to explain the properties of the impeding flow of the air into a heat sink. It is assumed that the flow is incompressible, buoyancy and radiation heat transfer effects are negligible and the thermodynamic properties are constant. If the flow variables are generalized in the form $f = \bar{f} + \acute{f}$ where $\bar{f}$ is the mean value and $\acute{f}$ is a fluctuation of the average, the continuity and Navier-Stokes equations can be written as follows:

$$\frac{\partial u_i}{\partial x_i} = 0 \tag{1}$$

$$\frac{\partial u_i}{\partial t} + \overline{u_j}\frac{\partial u_j}{\partial x_j} = \frac{1}{\rho}\frac{\partial \bar{P}}{\partial x_i} + \frac{\mu}{\rho}\nabla^2\overline{u_\iota} - \frac{\partial R_{\mathrm{ij}}}{\partial x_i} \tag{2}$$

where, x_i and x_j are the coordinate axes, t is the time, ρ is the density, $\bar{P}$ is the mean value of the pressure, μ is the viscosity, u_i is the velocity in i direction, u_j is the velocity in j direction, $\overline{u_\iota}$ is the mean value of velocity in l direction, $\overline{u_j}$ is the mean value of velocity in J direction, $\mathrm{R_{ij}}$ is the Reynolds stress term defined as:

$$-R_{ij} = \frac{\mu_t}{\rho}\left(\frac{\partial \overline{u_\iota}}{\partial x_j} + \frac{\partial \overline{u_j}}{\partial x_i}\right) - \frac{2}{3}\delta_{\mathrm{ij}}k \tag{3}$$

where, μ_t is the turbulent viscosity and k is the kinetic energy. It can be shown that the turbulent viscosity is proportional to the energy of the dissipation rate.

The mathematical modeling has been primarily employed to solve the source code addressing the energy of the dissipation rate (Eq. 4). The Ansys Fluent has been employed as the modeling software to implement the source term as subroutine. In this industrial research work the implementation of the mathematical modeling in the Ansys Fluent software is a critical part of the work aiming for design and optimization of the heat sink within SCI application. This can be presented as Eq. (4):

$$\frac{\mu_t}{\rho} = C_1\frac{k^2}{\varepsilon} \tag{4}$$

where, C_1 is a constant parameter and ε is the dissipation rate of turbulent energy. The energy equation which is solved for the conduction heat transfer within the heat sink is in the form of Eq. (5):

$$\rho C_P^s\frac{\partial T_s}{\partial t} = \frac{\partial}{\partial x_i}\left(k_s\frac{\partial T_s}{\partial x_i}\right) + \dot{q} \tag{5}$$

where, $\dot{q}$ is the generated heat per unit volume within the test chip, C_P^s is the specific heat capacity of the solid, k_s and T_s stand for the heat conductivity and temperature within the heat sink. The energy equation of the fluid flow is:

$$\rho C_P^l\frac{\partial \overline{T}}{\partial t} + \overline{u_\iota}\frac{\partial \overline{T}}{\partial x_i} = \frac{\partial}{\partial x_i}\left(k\frac{\partial \overline{T}}{\partial x_i} - \acute{T}\acute{u}\right) \tag{6}$$

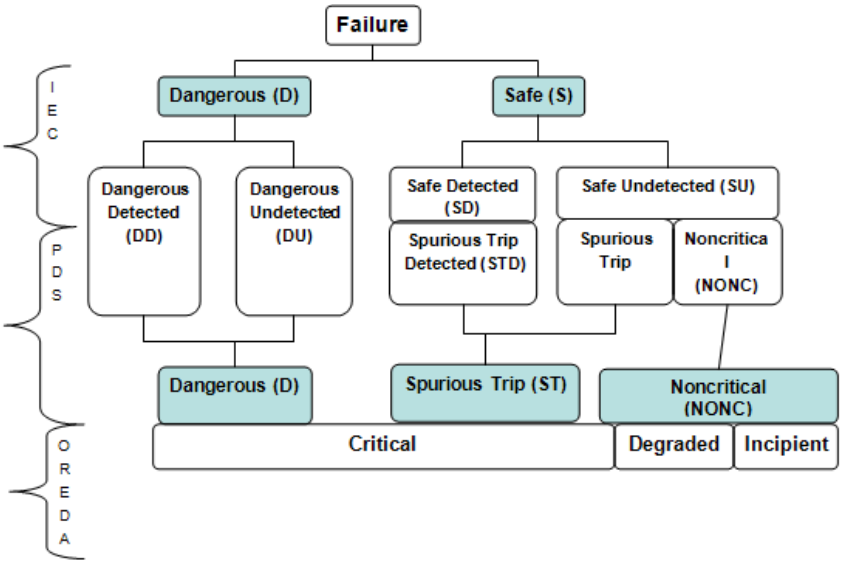

where, C_P^l is the specific heat capacity of the liquid, $\bar{T}$ is the time average of temperature, $\acute{T}$ is the temperature fluctuation, $\acute{u}$ is the velocity fluctuation.

2.2. Implementation procedure

In this section, the governing equations are discretized by using a finite-volume approach and solved by the SIMPLEC algorithm along with the usage of FLUENT. The accurate numerical modeling of this process requires a validated description of the boundary conditions, which tend to be in empirical form for this special case. The required boundary conditions used for the solution of Eqs. (1-6) are as follows: (1) no-slip wall condition, (2) energy conservation between the conduction and convection, (3) 45°C ambient temperature for P4_Standard (a case of the two considered heat sinks) and 39°C for P4_Special (another case of the heat sink), (4) 75W heat generated at the heat source, (5) thermal resistance of 0.35 K/W between the bottom plate and the copper plate that the heat sink is attached to, and (6) the soft soldering between the bottom plates and fins with $\rho = 7350\,kg/m^3$, $C_P = 229\,J/kgK$, and $k = 69\,W/mK$. Note that the components of velocity at the heat sink wall are assumed in no-slip boundary condition. Also, the continuity of the temperature and heat flux is utilized to couple the energy equations of the fluid and solid phases as the conjugate boundary condition.

2.3. Failure Mode Classification

Please note the following with respect to classification of critical failures:

OREDA classifies all failures into severity classes denoted critical, degraded and incipient (and unknown).

Note that critical failures can be split into dangerous (D) and spurious trip (ST), and further into detected and undetected. It displays the relation between the OREDA severity classes, and the IEC 61508 split into Dangerous and Safe, where Dangerous and Safe are sub-divided into Detected (SD) and Undetected (SU). In revised ISO 14224 the term “Severity” is renamed “Failure impact”.

The proposed methodology has been used and applied by on a Failure SIL analyses data study using the OREDA database.

Note that two components of SCM were not covered by the Failure mode classification given in the study proposal. These are:

- Industrial Heat sink as its standalone component
- Industrial Heat exchanger (as part of the industrial heat exchanger)

Failure mode classifications for these components have been set by extracting failure modes applicable in OREDA. Whether a given component with a given failure mode should be categorized as spurious trip or dangerous was set up based on IRIS expertise on subsea control systems. Naturally the judgement should be further agreed to be in line with industry expertise consensus.

The Failure mode classification used for the analysis:

- D means dangerous,
- ST means spurious trip,
- Split means that half the failures is considered dangerous while the other half is considered spurious trips,
- N/A means that the failure mode is not available for that component in OREDA,
- N/A N means that the failure mode is available for that component in OREDA, but the failure mode is NOT active.

Limitations and additional information regarding the failure mode classification methodology are presented in next section. The following chapters have been addressed:

- Conversion rules for failure detection method from OREDA to IEC 61508 conventions
- Failure mode classification for the selected components
- Failure mode classification and its limits & assumptions
- Failure rate analysis for use in SIL analysis
- Data source

To keep this report as short as possible, the details won’t be repeated here.

To initiate the implementation of SIL analysis, the development of a failure mode classification table is required. Based on the received information from the experts, such a table is created where relevant failure modes are classified for each of the selected components as Dangerous (D), Spurious Trip (ST), or Split. In determination of whether an arbitrary component with a given failure mode should be categorized as a ST or D, the experts’ opinion is taken into account. Also, this should be further assessed to be in line with the consensus of industry experts. Therefore, failure modes have been categorized for each component. Then, it was given to manufactures and some oil companies in order to receive comments and potential solutions on the proposed cross-mapping table. Finally, the comments have been evaluated and are approved by the committee. The final version of the critical failure mode classification is presented in Table 3. Note that while the procedure to provide the following table may seem similar to the FMEA method in some aspects, such as the identification of failure modes and determination of their severity class, it does not address the causes and effects of those failures. More information could be found in my other two papers.

Table 1. Thermal specification of the chosen system (Intel P4 processors)

Parameter	Value
Processor power dissipation	76 W
The maximum allowable temperature	67°C
Ambient air temperature	45°C
Thermal resistance	0.35C/W
Inlet velocity	duct with 3 m/s
Total heat sink height	25 mm

Table 2. Geometrical data of the Al-based heat sink

Case Intel P4	Dimension $w \times l \times d$ (mm)	Fin thickness (mm)	Fin pitch (mm)	Base thickness (mm)	IHS (mm)	Source (mm)
Special	61 × 80 × 37.9	0.4	1.5	12.9	31 × 31	15 × 15
Standard	72 × 90 × 25	0.25	1.5	5	31 × 31	15 × 15

Note: Since OREDA is not a SIL-analysis tool by nature, it has been earlier decided to construct definitions of STU for all practical purposes, i.e. STU has been defined based on mapping tables (for Detection method and Failures modes per component. A similar strategy could be found elsewhere [62-64].

3. Validation of the Model

In order to validate the proposed model, as described in the previous section, aluminum heat sinks are chosen and analyzed for an Intel P4_Standard system with the thermal design specifications presented in Table 1. A typical Al-based heat sink is shown in Fig. 1 as well.

It is intended to compare the model's predictions with those obtained from the experimental data of various operational parameters of an Al-based heat sink with a density of 2700 kg/m^3. It is manufactured by the compressive extruded plates with a thermal conductivity of around 220 W/m·K. The bottom plate of the heat sink is assumed as a homogenous material and its thermal resistance with the heat source is negligible. Also, the impact of the heat sink's edge surfaces is ignored and it is assumed that the heat source generates uniform heat flux. The geometrical data are given in Table 2 as well. In this table, IHS stands for the Integrated Heat Spreader.

This provide the opportunity to compute different BC/IC in relation to the source term effect in which is the heat of the article.

It should be noted that the mentioned results have been employed for the validation purpose of the CFD model. The source data has been computed using in house subroutine in which implemented to the Ansys Fluent environment.

The results (section 4) present the industrial approach of the implementation of the in house developed CFD method to analyses the energy of the dissipation rate of exemplary industrial heatsink with special focus in the subsea control system.

The results in the section 4 are generic data from different exemplary industrial measurements available in the cloud solution. Besides, the confidentiality of the information is preserved, that is, all industrial data have been presented in a way which prevents the dissemination of industrial confidential information. To secure this purpose, all data have been generalized and normalized to avoid the exposure of any possible confidential information.

4. Results

It should be noted that the heat source is mounted centrally on the base plate and the heat sink is cooled evenly across the exposed finned surface. Moreover, all the heating power is conducted to the fins so that the external heat losses can be neglected. The contribution of the radiation is negligible as well due to a relatively small temperature difference. Also, the Reynolds number of the flow rate in the channel of heat sink indicates that the turbulent flow should be considered. The computational domain of this study is given in Fig. 2.

The intake fan of the correct size and power is used on top of the heat sink. The air coolant enters to the heat sink from the top surface at a constant temperature. The fan is characterized by depicting the variations of the flow rate with respect to the pressure drop, shown in Fig. 3. Obviously, the temperature variations associated with the airflow depends on the flow resistance of the heat sink. A pressure drop of 0.1 in H_2O or 24.5 Pa leads to the production of around 11 CFM flow rate in 4.2 m/s.

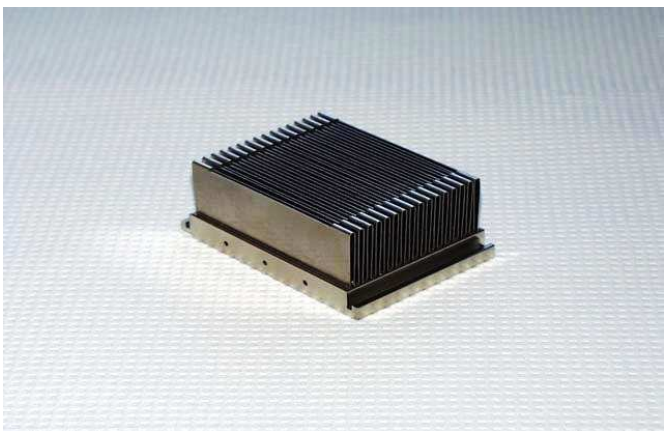

Fig. 1. Typical Al-based heat sink for Intel P4_Standard

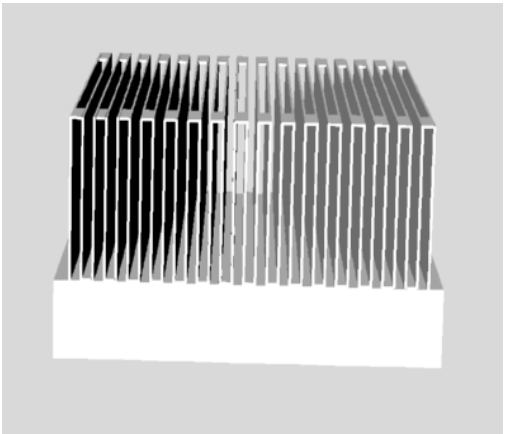

Fig. 2. Computational domain for P4_Special

Table 3. Results of the simulation for Al-based heat sink

Parameter	Value
Volume (Bottom, Al plate, fins)	8.726603e-5 m^3
Weight	235.618 g
Mass flow rate of the fan	0.0118 kg/s
Generated Heat of the heat source	76 W
Outlet flow rate	2(0.0056) = - 0.0118 kg/s
Mass weighted average of the fan	3.72 m/s
Facet average of the heat transfer coefficient in heat source	482.3062 W/m^2k
Facet average of the heat flux in heat source	23087.97 W/m^2
Average of the total pressure drop between the fan and outlet	31.9 Pascal
Size of the heat sink	61 × (25 + 12.9) × 80 mm
Size of the fin	0.4 mm × 25 mm
Size of the fin pitch	1.5 mm

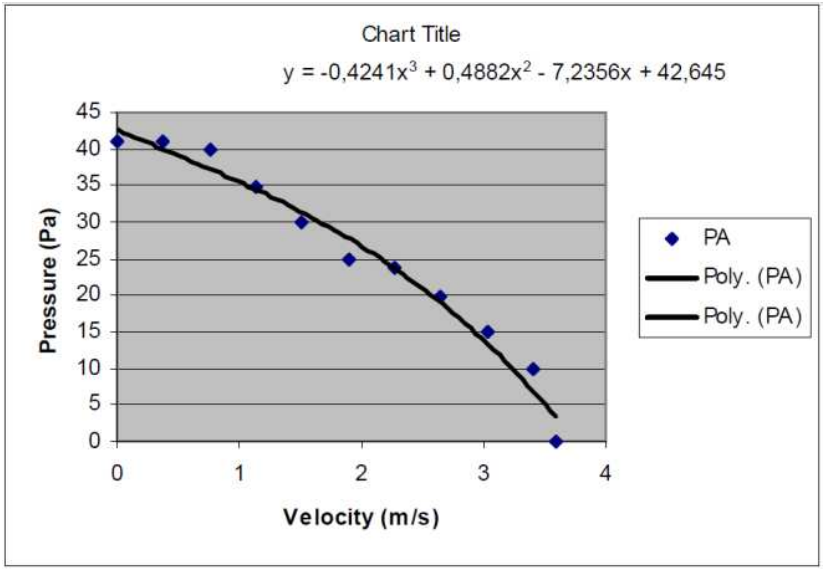

Fig. 3. Variations of the flow rate with respect the pressure drop

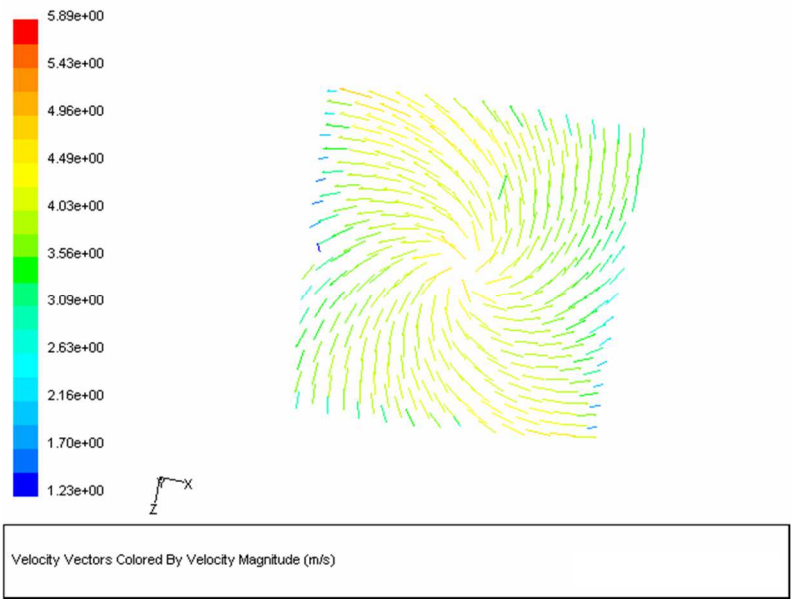

Fig. 4. Fan characteristic curve

Based on Fig. 3, the fan characteristic curve follows a polynomial formula shown as Eq. (7) which is obtained by curve fitting of the experimentalpoints. This equation provides the simulation of fan behavior presented in Fig. 4, in which x and Y represent the horizontal and vertical axes, respectively.

$$Y = -0.4241x^3 + 0.4882x^2 - 7.2356x + 42.645 \tag{7}$$

Figures 5-8 show respectively the velocity distribution of the domain, temperature distribution of the heat source and fins connection, temperature distribution of the Al-based heat sink, and the temperature distribution of the bottom plate. The temperature varies between 300-337 K at the heat source.

It can be concluded that the prediction of the thermal parameters from simulations is within acceptable limits compared to those reported earlier. The results can be summarized as Table 3.

Hence, the validity of the presented model is completed by comparing the predicted results with the available measured data which is based on the author's works in [41-55]. It should also be mentioned that, as seen in the referred reports, this work has a rich experimental background. That is, it is based on numerous years of research on various aspects of aluminum and copper metals such as the welding, brazing, and casting. Moreover, the author has more than a decade of practical experience in working with these metals in various applications, such as those published in [56-61] and the above cited industrial reports. Hence, the model is reliable and applicable for the thermal design and assessment of the Cu-based heat sinks as addressed in the following sections.

4.1. Analysis of Cu-based Heat Sinks

In this section, it is intended to employ the proposed model for the analysis of Cu-based heat sinks with a density of 8900 kg/m^3, which was validated for aluminum ones. Two configurations are considered and distributions of the velocity and temperature as well as values of some parameter are obtained.

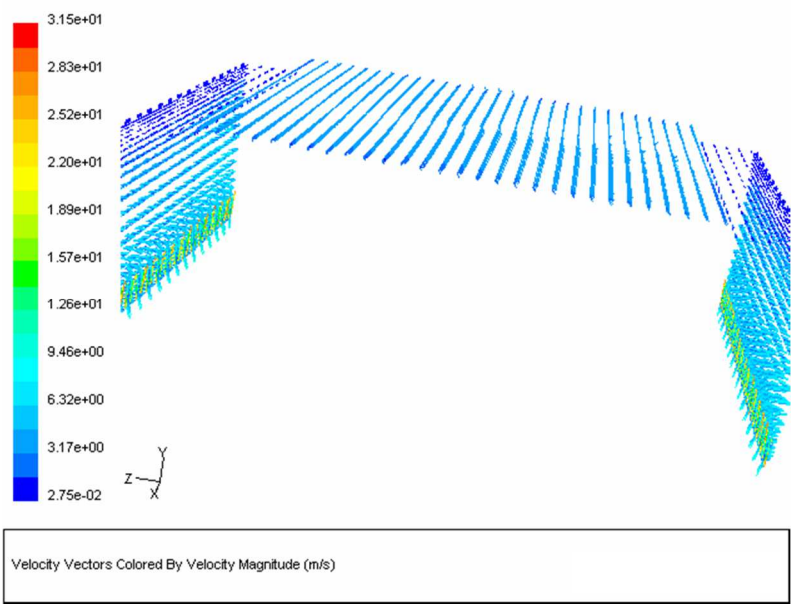

Fig. 5. Velocity distribution of the domain of the Al heat sink

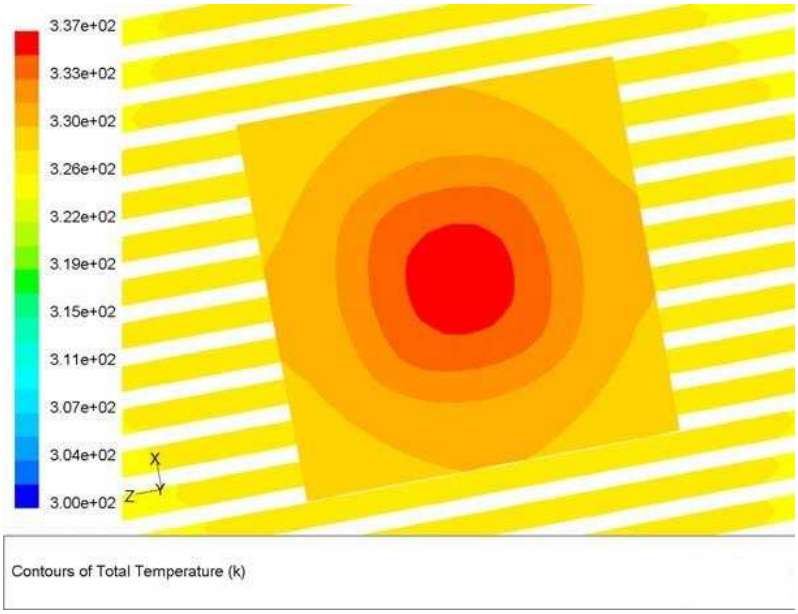

Fig. 6. Temperature distribution of the heat source and fins connection of the Al heat sink

Table 4. The geometrical data of P4 special

Intel P4 Special	Dimension w x l x d (mm)	Fin t (mm)	Fin pitch (mm)	Base t (mm)	IHS (mm)	Source (mm)
Case 1	60 × 50 × 25	0.25	1.5	5	31 × 31	15 × 15

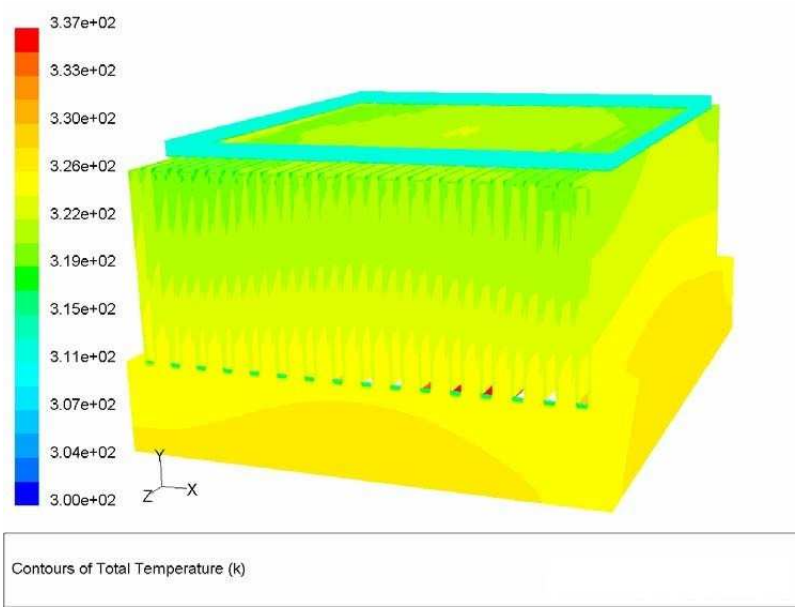

Fig. 7. General view of the temperature distribution of the Al heat sink

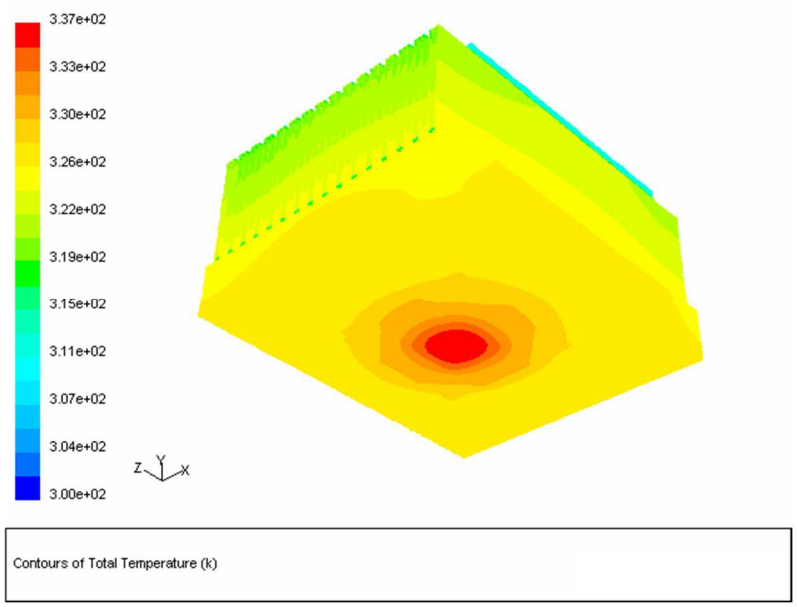

Fig. 8. Temperature distribution of the bottom plate of the Al heat sink

4.2. Rectangular heat sink based on straight fins

It is reported previously in [40] that rectangular heat sinks based on the straight fins have high potential for application in thermal management of the electronic packages. This design is compact and light enough, and is capable of dissipating a significant thermal load with a relatively small increase in the package temperature. It was also found in the referred work that a thickness of around 3.5-5 mm for the bottom plate and around 0.25 mm for the fins looks to be the optimum values. Now, it is aimed to replace the analyzed aluminum heat sinks with the copper ones in a three-dimensional rectangular symmetric heat sink with the following geometrical data known as case1_Special:

The results are presented in Figs. 9-13 including the distribution of temperature and velocity.

Figure 9 shows the distribution of velocity in the Cu-based heat sink. The velocity varies along the y-axis from almost 0.79 to 9.1 m/s with the maximum value at the top. Note to the local variation of the velocity both in the inlet and outlet. Based on the above figures, it is seen that the highest temperature for the copper case is in about 340 K, which is an acceptable value. The values of parameters are resulted as Table 5.

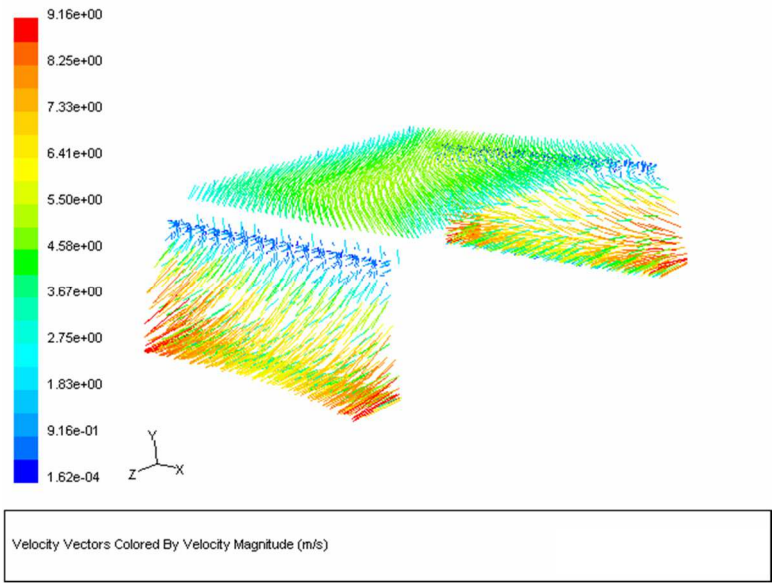

Fig. 9. Domain velocity distribution of the first case

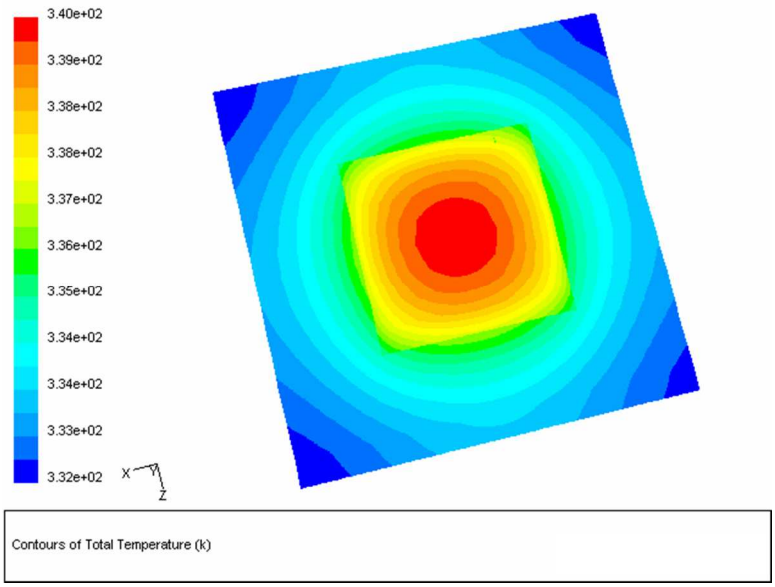

Fig. 10. Temperature distribution in the heat source of the first case

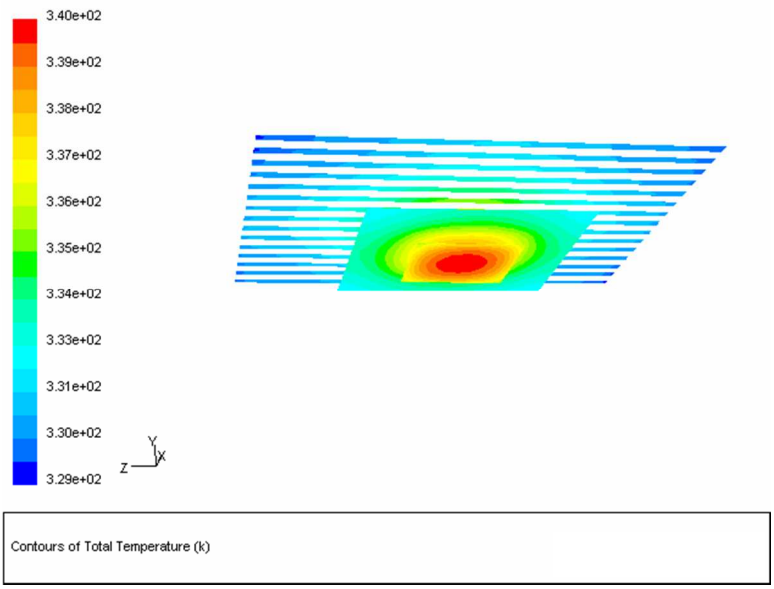

Fig. 11. Temperature distribution in fin connection of the first case

Table 5. Results of the simulation for Cu-based heat sink

Parameter	Value
Volume (Bottom, copper plate, fins)	2.611275e-5 m^3
Weight	232 g
Mass flow rate of the fan	0.0090 kg/s
Generated Heat of the heat source	76 W
Outlet flow rate	2(0.0045) = - 0.0090 kg/s
Mass weighted average of the Fan	4.16 m/s
Facet average of the heat transfer coefficient in heat source	6702.508 W/m^2k
Facet average of the heat flux in heat source	337777 W/m^2
Average of the total pressure drop between the fan and outlet	29.3 Pascal
Size of the fin	0.25 × 20 × 50 mm
Size of the fan block	4 mm

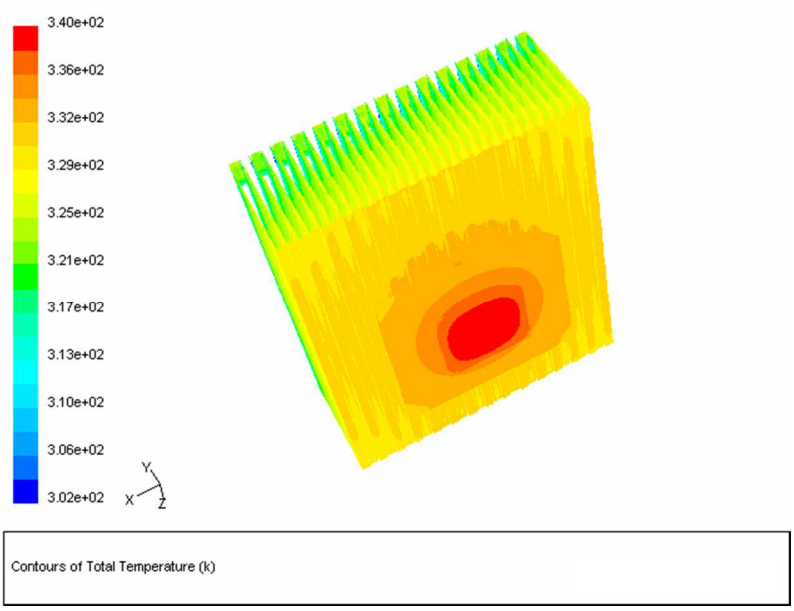

Fig. 12. Overall temperature distribution of the first case

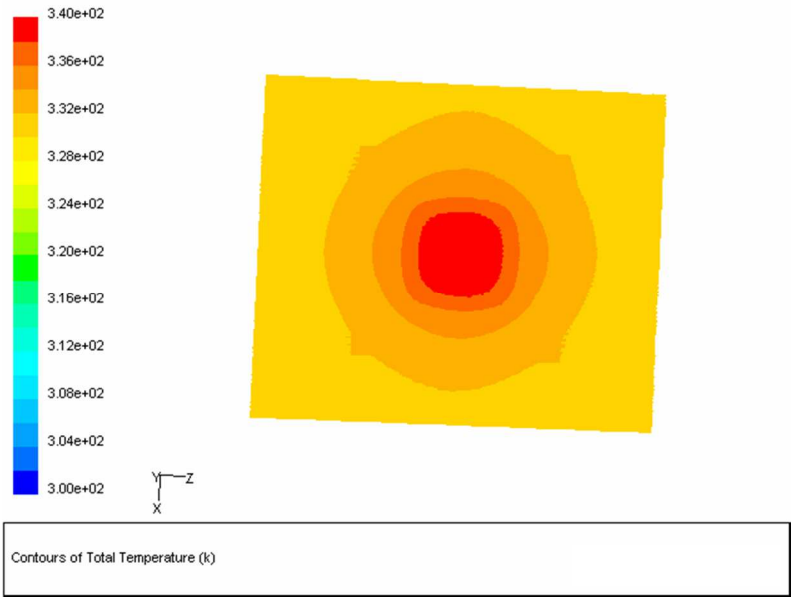

Fig. 13. Bottom view of the first case

As seen in Table 5, the thickness of the bottom plate is just 5 mm and the fin height is 20 mm. However, for Al-based heat sinks, these values are respectively 12.9 and 25 mm. Also, the spreading of the heat in copper case is faster than the Al one in all coordinate directions. This is due to the transfer of the supplied heat along the fins. In fact, it dissipates from the interface of the fin and fluid gradually leading to the creation of a familiar negative temperature gradient in the longitudinal direction of the fins. Then, the cooling air is directed to flow in the transverse direction. Moreover, the outlet air temperature can be noticeably higher than the inlet one. Hence, the end part of the fin results in less heat dissipation than the starting one. The findings show that:

Table 6. The geometrical data of P4 special

Intel P4 Special	Dimension $w \times l \times d$ (mm)	Fin t (mm)	Fin pitch (mm)	Base t (mm)	IHS (mm)	Source (mm)
Case 2	72 × 90 × 25	0.1	3.67	5	31 × 31	15 × 15

- Based on the thermal field analysis, the isotherms are closely packed everywhere and can gradually be dispersed during the simultaneous increase of the air region temperature.
- The transferred heat between the solid and air reaches its maximum value near the source of the heat and the base plate.
- The resulted heat flux from the heat source can immediately be dispersed through the bottom substratum by conduction. It has eventually been transferred through all the fins to the air in a roughly uniform way.

The thermal development region does not occupy essentially the entire length of the fins owing to the conjugate convection-conduction interaction. This can be a positive sign for smaller heat sinks at least in the z-direction and in more conductive material like copper. It can also be seen that the average $\bar{h}$ at the heat source surface is much higher for the copper case. All in all, it is concluded that considering a heat sink with smaller dimensions may yield sufficient amount of the cooling rate to scatter 70 W from the heat source.

4.3. An Automotive-based heat sink without louver

In this section, the proposed model is utilized to analysis another heat sink design. This is an automotive based heat sink without louver which is shown schematically in Fig.14. The related geometrical data are provided in Table 6 known as Case 2.

In a similar way to the previous case, the temperature and velocity distribution are evaluated and compared with the heat and mass flux (of what from which case?) with the aim of identifying the thermal performance. The computations are carried out using the similar operating parameters. The results are provided in Figs. 15-17.

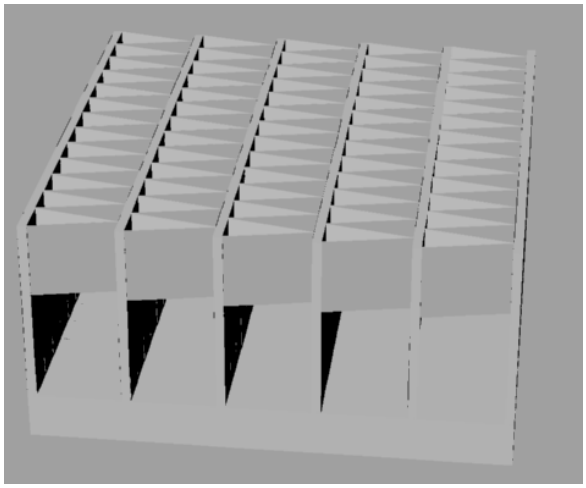

Fig. 14. Automotive based heat sink without louvers

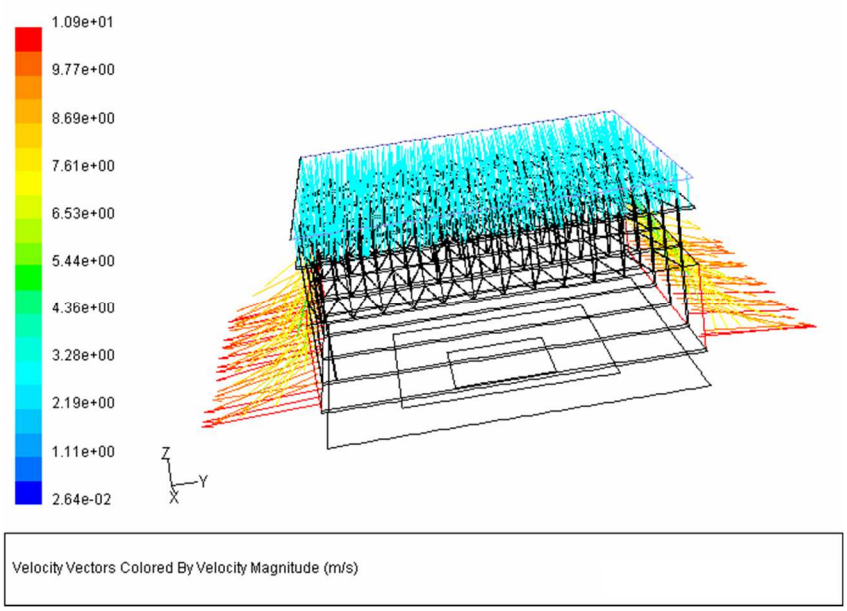

Fig. 15. Domain velocity distribution the second case

Table 7. Results of the simulation for Cu-based heat sink

Parameter	Value
Volume (Bottom, copper plate, fins)	2.0797e-5 m^3
Weight	184 g
Mass flow rate of the fan	0.02915 (m/s) (kg/s)
Generated Heat of the heat source	76 W
Outlet flow rate	2(0.0045) = - 0.0090 kg/s
Mass weighted average of the Fan	3.0 m/s
Facet average of the heat transfer coefficient in heat source	5072 W/m^2k
Facet average of the heat flux in heat source	337777 W/m^2
Average of the total pressure drop between the fan and outlet	64 Pascal
Size of the heat sink	50 × 50 × 25 mm
Size of the fin	0.25 × 20 × 50 mm
Size of the fan block	4 mm
Thickness of the holder	0.5 mm

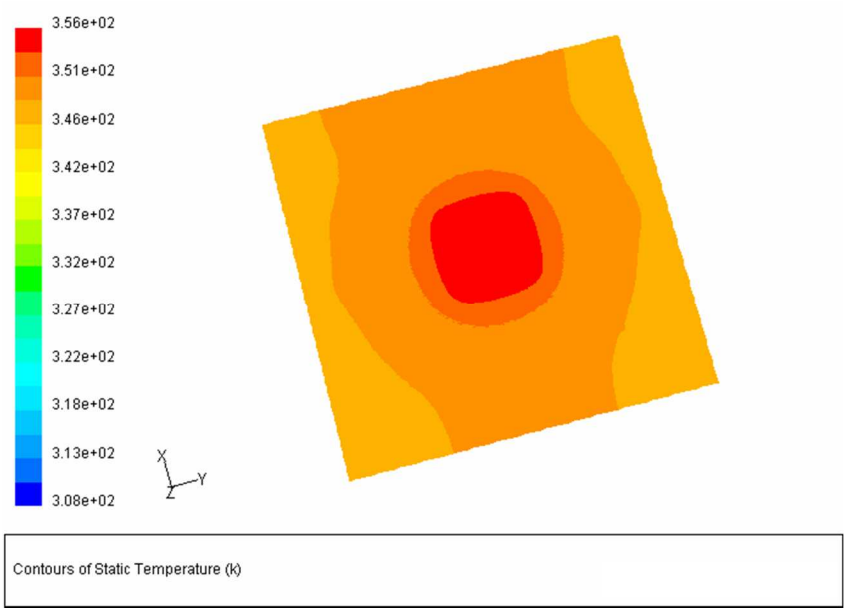

Fig. 16. Bottom plate temperature field of the second case

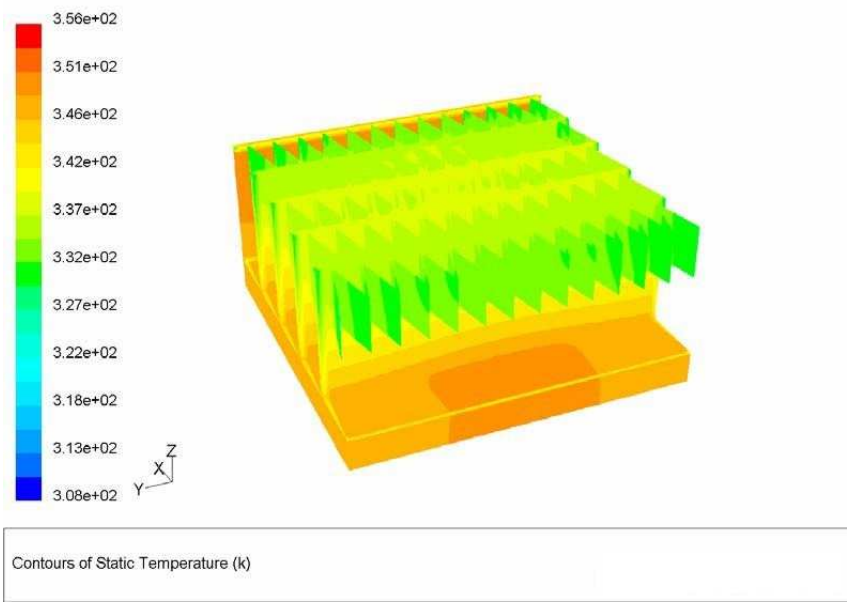

Fig. 17. General temperature field of the second case

Table 8. The geometrical data of P4 standard – Case 3

Intel P4 Standard	Dimension $w \times l \times d$ (mm)	Fin thickness (mm)	Fin pitch (mm)	Base t (mm)	IHS (mm)	Source (mm)
Case 3	72 × 90 × 25	0.25	1.5	5	31 × 31	15 × 15

Figures 15-17 show the velocity and temperature distribution of the entire unit cell. The results are comparable to those presented earlier in Figs. 9-13. It is seen that the changes of velocity are more noticeable under the inlet fan which is not subjected to the flow. Also, the changes of temperature are more intense near the bottom plate, which is the area of heat generation. Evaluating the distributions of temperature and velocity for the second case represents a large dependence on the intake fan position. This has been discussed earlier [3]. Moreover, it is resulted that the flow behavior highly affects the distribution of temperature, velocity, and heat flux in the unit cell of heat sink. This effect is common in different cases. Hence, the results of parameters are summarized in Table 7.

The provided values represent that for the maximum efficiency of a triangle-based heat sink, the flow has to pass through the fins. Besides, a side-mounted fan will yield a greater cooling effect, which is investigated below as P4_Standard case.

5. Discussion

In this section, it is aimed to use and discuss the previous results for optimizing the Cu-based heat sinks by considering various changes in parameters such as the thickness. A simple analytical estimation shows that it is quite difficult to make the heat sink based on the thermal specifications in Table 1. The absolute maximum heat that can be dissipated in this case will be:

$$Q = \rho . C_p . A . v . \Delta T \tag{8}$$

where, A stands for the flow cross-section area, v is the velocity, and ΔT is the temperature change of the air. Substitution of the values leads to the following result:

$$Q = 1.225[kg/m^3] \times 1000[J/kgK] \times (0.072 \times 0.020)[m^2] \times 3[m/s] \times (67 - 45)[K] = 116.W$$

That's the case for an ideal situation with fin effectiveness of 100%, which is far from the real case.

Hence, the problem is to minimize the thermal interaction between a coolant stream (U_0, T_0) and a certain space volume $(L \times H \times W)$ where heat is generated at the rate of q. The overall thermal resistance is $q/(T_{max} - T_0)$, where T_{max} is the highest temperature occurring at the center of the heat source surface.

In order to optimize the overall heat sink, thermal performance should be maximized and weight-satisfying constraints (dimension, manufacturing) should be minimized [62]. The performance of a heat sink is measured by the temperature difference between the base of the heat sink and the ambient air temperature. The objective of the optimization is to minimize the weight and volume of the heat sink and to fulfill the temperature constraints of the heat dissipation. For this purpose, two cases are considered as follows:

5.1. Rectangular heat sink based on the straight fins (Case 3)

The first considered design is the rectangular heat sink based on straight fins with a 5 mm thickness of the bottom plate, 0.25 mm thickness of the fins and fin pitch of 1.5 mm as seen in Table 8. The related computational domain is given in Fig. 18 as well. As seen, the dimensions of the heat sink are changed.

The square specimen was selected to consider the effect of Thermal Barrier Coating (TBC) systems in practical application. It is used to insulate the metal substrates from high-temperature oxidation and corrosive environments on diesel components such as the valves, pistons and fire decks. It also reduces the non-occurrence metal temperatures as a thermal barrier.

Based on the analyses, the gradual weight loss was observed after 52 cycles indicating the thermal degradation of coated specimens. Moreover, the sudden weight loss of the samples was observed after 97 cycles, implying the damage to the coating through the cracking mode. During the cooling process, the successful design of the copper heat sinks requires a basic understanding of the transport methods. To design the lightweight ones, efficient and reliable thermal management systems, precise measurements and forecasts of the local temperature as well as the heat fluxes are of paramount importance. The local temperature, heat and mass flux will be examined with the aim of identifying the thermal performance addressed in the three potential unit cells of the Cu-based heat sinks, shown in Fig. 2. The results are shown in Figs. 19-22 and Table 9.

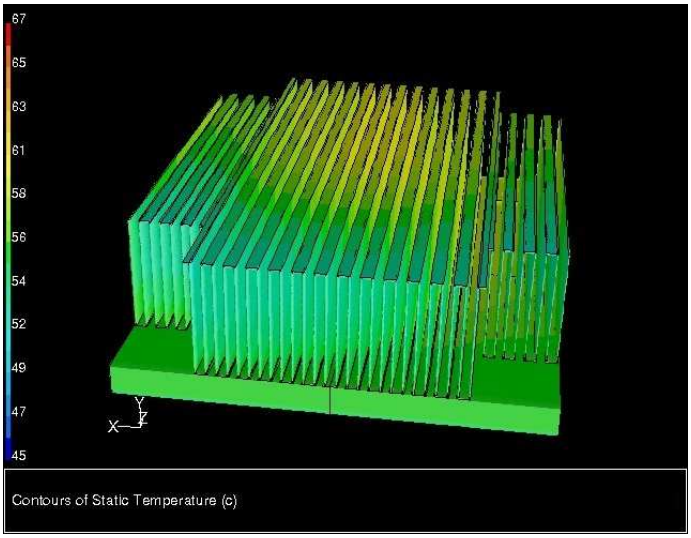

Fig. 18. Computational domain of the third case

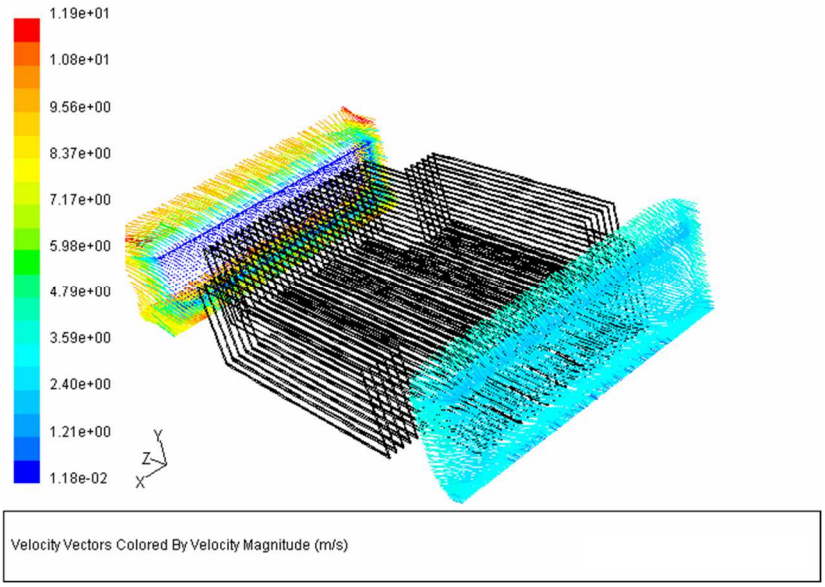

Fig. 19. Domain velocity pattern of the third case

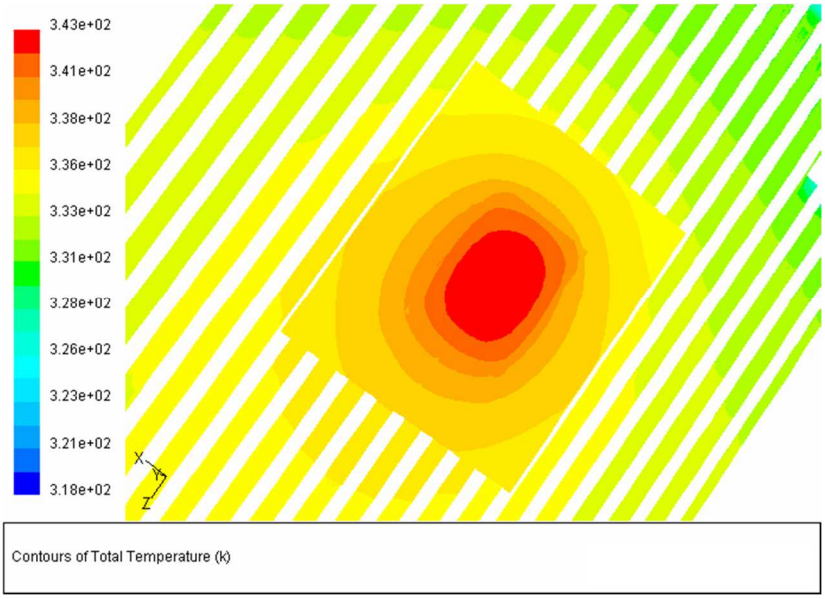

Fig. 20. Temperature distribution in heat source of the third case

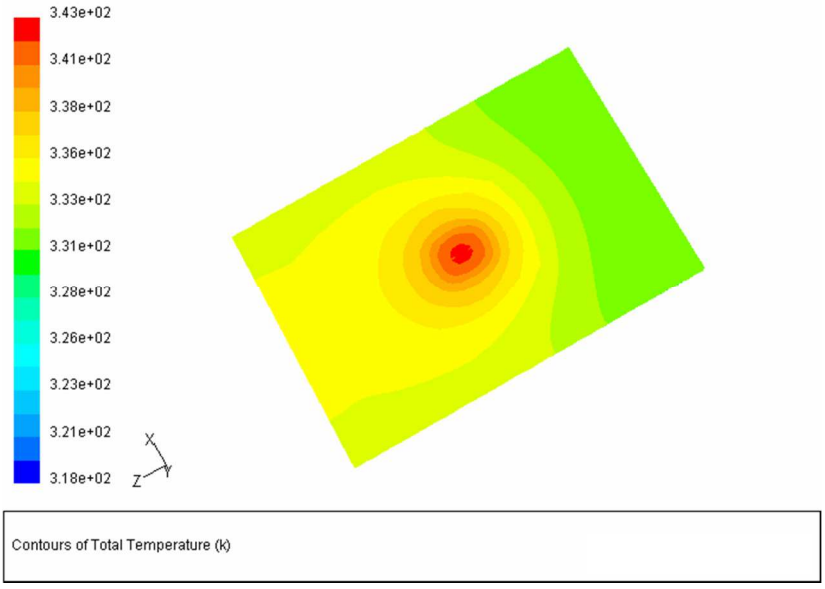

Fig. 21. Bottom plate temperature distribution of the third case

Table 9. Results of the simulation for Cu-based heat sink – Case 3

Parameter	Value
Volume (bottom, copper plate, fins)	2(2.619544e-5) m^3
Weight	470 g
Mass flow rate of the fan	0.0032 kg/s
Generated heat of the heat source	75 W
Outlet flow rate	2(0.0056) = - 0.0032 kg/s
Mass weighted average of the fan	3.0 m/s
Facet average of the heat transfer coefficient in heat source	7528.45 W/m^2k
Facet average of the heat flux in heat source	23087.97 W/m^2
Facet Average of the heat flux at fin surfaces	13.56 W/m^2K
Average of the total pressure drop between the fan and outlet	79.4 Pascal

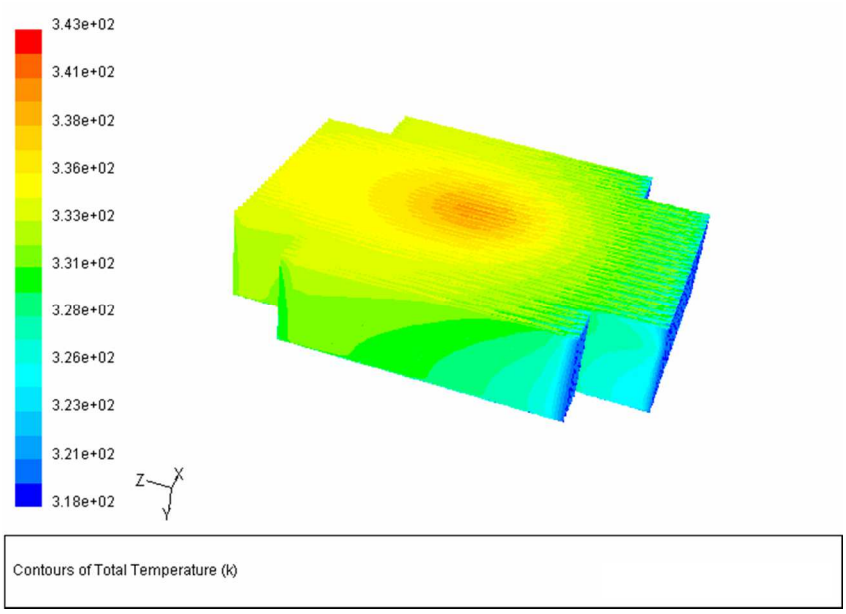

Fig. 22. General temperature distribution of the third case

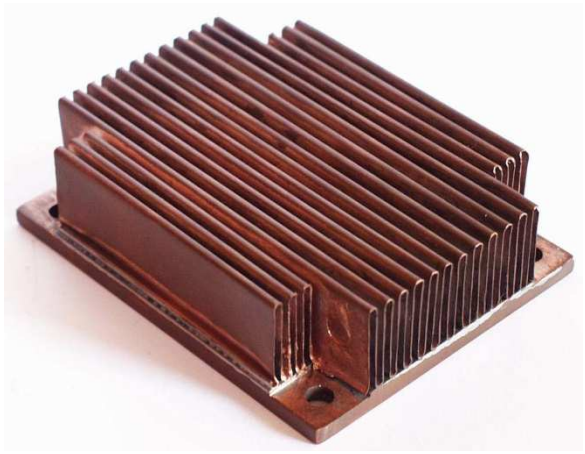

Fig. 23. Sample made for the third case test

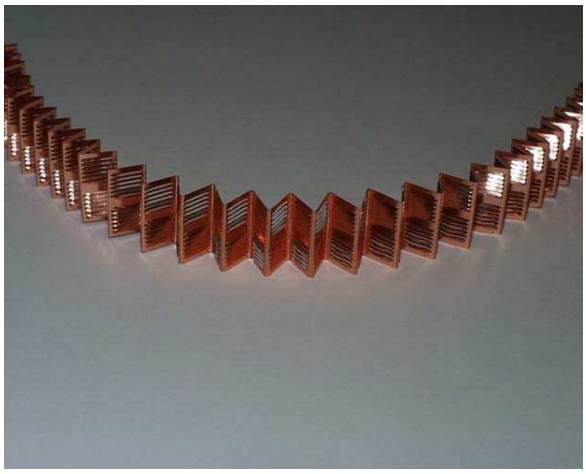

Fig. 24. A sample type of the louvered fins

The analyses suggest that the rectangular heat sink with the straight fins has a high potential to be used in thermal management of the electronic packages. This concept must be examined with some experimental studies to quantify its behavior. Fig. 23 shows a sample made for the test.

5.2. Automotive-based design (Case 4)

It was earlier discussed that the automotive-based heat sink shows a great dependency with respect to the intake fan position. The highest efficiency will be achieved when the flow has to pass through the fins. Also, a side-mounted fan yields a larger cooling effect. The problem might be the convection effect in dissipating the heat from the source. This requires decreasing the fin thickness as well as possible increase of the number of the fins. It will have a negative effect on the conduction mechanism and the pressure resistance of the sample.

Table 10. The geometrical data of P4 standard – Case 4

Intel P4 Standard	Dimension w x l x d (mm)	Fin thickness (mm)	Fin pitch (mm)	Base t (mm)	IHS (mm)	Source (mm)
Case 4	72 × 90 × 25	0.05	3.67	5	31 × 31	15 × 15

Based on the above explanations, it is intended to use louvered fins, such as the sample one shown in Fig. 24, to: (1) modify the convection effect, (2) increase the fin (heat transfer) efficiency and (3) to avoid the large increasing of the pressure drop. Therefore, the simulation needs to be employed as a designing tool to optimize the fin profiles (in terms of thickness, number of fins and fin pitch) and to optimize the louver performance in terms of size, angle and number. The related geometrical data of this case are presented in Table 10. Also, note that the curvature of the louvered-fin makes it difficult to accurately model the fine geometry, as the required grid size would be very small, resulting in long solution time.

Figures 25 indicate two possible heat sink designs with different fin pitches. Figure 26 illustrate another design which could be considered as a combined design of cases 3 and 4. The computation results for those will be discussed in the upcoming works of the author.

To improve the failure rates, some measures can be taken, such as (1) proper installation of the heat exchanger/ heat sink components, which can be useful in the prevention of failure modes such as the leakage, (2) modification or improvement of the components' materials, which is helpful in overcoming failure modes like the failing of the component to function on demand, and (3) enhancement of subsea design.

This requires the adoption of measures such as the implementation of RAM (Reliability, Availability, and Maintainability) analysis as early as possible to make the potential design changes in a low cost and to provide a sound background for further decisions on the inspection, maintenance, repair and etc.

To provide a better insight into the above results such as values of parameters, their graphical representations are shown in Figs. 9-25 and tables 4-10. This helps a better comprehension of results. Also, the values of different parameters are compared with a different version of a typical heat sinks material and configuration in which could be employed at SCS application through OREDA database [63-64]. The comparisons of different heat exchanger component inventory values for two versions of the OREDA database indicated elsewhere [63-64].

These results should be used as a guide for failure rates. To improve failure rates, some measures can be taken, such as proper installation of the Heat sink components, which can be useful in the prevention of failure modes such as the leakage, modification or improvement of the components' materials, which is helpful in overcoming failure modes like the failing of the component to function on demand, and enhancement of subsea design.

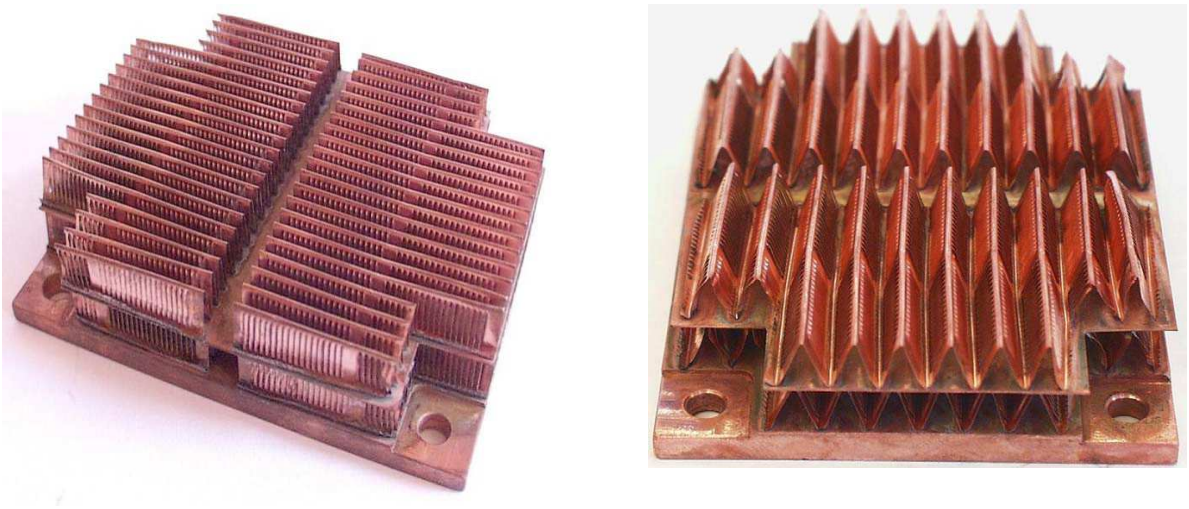

Fig. 25. Two possible heat sink designs with different fin pitches, (a) high dense fin, (b) low dense fin

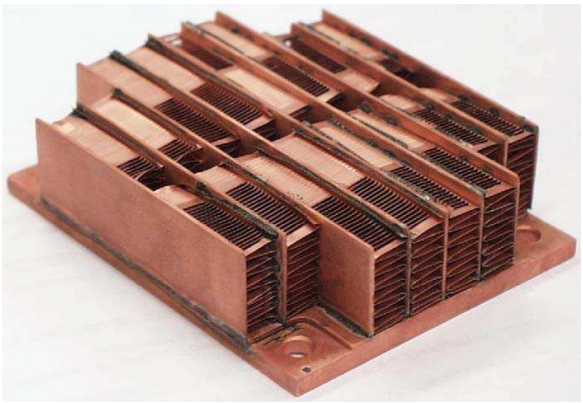

Fig. 26. A combined design of cases 3 & 4

6. Conclusion

In this work, a mathematical model was used for heat sinks aiming to increase their heat release as well as to decrease their volume. The model was proved to be capable of usage for both aluminum and copper heat sinks. Also, the effects of various changes in geometrical design of the Cu-based heat sinks, such as the change of fin pitch, were studied. The results show that the model is capable of simulating both the aluminum and copper heat sinks. In fact, the present study succeeds in illustrating the utilization of mathematical modeling in both refining a heat sink configuration and giving the practical insight into the flow and heat transfer properties of a heat sink. The proposed procedure of SIL analysis included the development of failure mode classification tables, evaluation of several parameters such as failure events, and calculations of failure rate for a selection of Heat Exchanger (including Heat Sink) components in SCS. Also, the dominant failure modes were identified as control/signal failure and fail to function on demand. Furthermore, failure rate of SEM led to the highest values of critical failure rates. The developed SIL can be highly useful in the prevention or mitigation of the consequences of heat sink failure occurrences. These could be a huge loss in production, environmental issues, and uneconomical field developments with substantial safety risks. Hence, the work tried to provide an appreciable contribution in the area, which has been implemented in practice with satisfactory results. As a suggestion, future study of the topic could be the investigation of specific degradation of materials over time in harsh environments. A general approach is to begin with systematic characterization of the degraded material's sensitivity to temperature, pressure, flow condition, and chemical environment, both dependently and independently. The time factor (i.e. aging over time) is also an influential factor in this respect. Evaluation of different structures in the database (topsea vs. subsea) is another suggested future work.

Author Contributions

The author discussed the results, reviewed, and approved the final version of the manuscript.

Acknowledgments

This work has been conducted in the framework of the Outokumpu Copper, Sweden/ Finland, when the author held the position of a Global R&D manager there. The paper is based on an industrial work in which the author acted as the project manager. It should be noted that the work presents the academic approach of the implementation of the CFD method to analyse the energy of the dissipation rate of an industrial heatsink with special focus in the subsea control system. The mentioned data in the paper are generic data from different exemplary industrial measurements available in the cloud solution. Besides, the confidentiality of the information is preserved, that is, all industrial data have been presented in a way which prevents the dissemination of industrial confidential information. To secure this purpose, all data have been generalized and normalized to avoid the exposure of any possible confidential information.

Conflict of Interest

The author declared no potential conflicts of interest concerning the research, authorship, and publication of this article.

Funding

The author received no financial support for the research, authorship, and publication of this article.

Data Availability Statements

The datasets generated and/or analyzed during the current study are available from the corresponding author on reasonable request.

References

[1] S. Sadrabadi Haghighi, H.R. Goshayeshi, M.R. Safaei, Natural convection heat transfer enhancement in new designs of plate-fin based heat sinks, *International Journal of Heat and Mass Transfer*, 125, 2018, 640-647.
[2] J. Chang, C. Yu, R. Webb, Identification of minimum air flow design for a desktop computer using CFD modeling, *Journal of Electronic Packaging*, 123(3), 2001, 225-231.
[3] M.R. Attar, M. Mohammadi, A. Taheri, S. Hosseinpour, M. Passandideh-Fard, M. Haddad Sabzevar, A. Davoodi, Heat transfer enhancement of conventional aluminum heat sinks with an innovative, cost-effective, and simple chemical roughening method, *Thermal Science and Engineering Progress*, 20, 2020, 100742.
[4] K. Zulfiqar, H. Muhammad Ali, Air cooled heat sink geometries subjected to forced flow: A critical review, *International Journal of Heat and Mass Transfer*, 130, 2019, 141-161.
[5] F.P. Incropera, Convection heat transfer in electronic equipment cooling, *Journal of Heat Transfer*, 110, 1988, 1097-1111.
[6] W. Nakayama, Thermal management of electronic equipment: a review of technology and research topics, *Applied Mechanics Reviews*, 39, 1986, 1847-1868.
[7] O. Sevgin, R. Hannemann, A. Bar-Cohen, High heat from a small package, *Mechanical Engineering*, 108, 1986.
[8] A. Bar-Cohen, Thermal management of electronic components with dielectric liquids, *JSME International Journal Series B Fluids and Thermal Engineering*, 36(1), 1993, 1-25.
[9] H.T. Dhaiban, M.A. Hussein, The Optimal Design of Heat Sinks: A Review, *Journal of Applied and Computational Mechanics*, 6(4), 2020, 1030-1043.
[10] S.Y. Kim, R.L. Webb, Thermal performance analysis of fan-heat sinks for CPU cooling, *In ASME International Mechanical Engineering Congress and Exposition*, 37181, 2003, 235-243.
[11] D. Kim, S.J. Kim, Thermal optimization of microchannel heat sink with pin fin structures, *ASME International Mechanical Engineering Congress and Exposition, American Society of Mechanical Engineers Digital Collection*, 593-602, 2003.
[12] K.K. Sikka, K.E. Torrance, C. Scholler, P. Salanova, Heat sinks with fluted and wavy plate fins in natural and low-velocity forced convection, *IEEE Transactions on Components, Packaging and Manufacturing Technology*, 25(2), 2002, 283-292.
[13] M.A.R. Junaidi, R. Rao, S.I. Sadaq, M.M. Ansari, Thermal analysis of splayed pin fin heat sink, *International Journal of Modern Communication Technologies & Research*, 2(4), 2014, 48-53.
[14] S.J. Kim, D.-K. Kim, H.H. Oh, Comparison of fluid flow and thermal characteristics of plate-fin and pin-fin heat sinks subject to a parallel flow, *Heat Transfer Engineering*, 29(2), 2008, 169-177.
[15] Y.-T. Yang, H.-S. Peng, Numerical study of thermal and hydraulic performance of compound heat sink, *Numerical Heat Transfer, Part A: Applications*, 55(5), 2009, 432-447.

[16] Z. Feng, I. Catton, Numerical evaluation of flow and heat transfer in plate-pin fin heat sinks with various pin cross-sections, *Numerical Heat Transfer, Part A: Applications*, 60(2), 2011, 107-128.
[17] H.E. Ahmed, B.H. Salman, A. Sh Kherbeet, M.I. Ahmed, Optimization of thermal design of heat sinks: A review, *International Journal of Heat and Mass Transfer*, 118, 2018, 129-153.
[18] X. Hui, Z. Liu, W. Liu, Conjugate heat transfer enhancement in the mini-channel heat sink by realizing the optimized flow pattern, *Applied Thermal Engineering*, 182, 2021, 116131.
[19] M.L., Elsayed, O. Mesalhy, J.P. Kizito, Q.H. Leland, L.C. Chow, Performance of a guided plate heat sink at high altitude, *International Journal of Heat and Mass Transfer*, 147, 2020, 118926.
[20] Z. Duan, X. Lv, H. Ma, L. Su, M. Zhang, Analysis of Flow Characteristics and Pressure Drop for an Impinging Plate Fin Heat Sink with Elliptic Bottom Profiles, *Applied Sciences*, 10(1), 2020, 225.
[21] X. Meng, J. Zhu, X. Wei, Y. Yan, Natural convection heat transfer of a straight-fin heat sink, *International Journal of Heat and Mass Transfer*, 123, 2018, 561-568.
[22] S. Huang, J. Zhao, L. Gong, X. Duan, Thermal performance and structure optimization for slotted microchannel heat sink, *Applied Thermal Engineering*, 115, 2017, 1266-1276.
[23] M.A. Alfellag, H.E. Ahmed, A. Sh Kherbeet, Numerical simulation of hydrothermal performance of minichannel heat sink using inclined slotted plate-fins and triangular pins, *Applied Thermal Engineering*, 164, 2020, 114509.
[24] K.S. Ong, C.F. Tan, K.C. Lai, K.H. Tan, Heat spreading and heat transfer coefficient with fin heat sink, *Applied Thermal Engineering*, 112, 2017, 1638-1647.
[25] J. Xu, Y. Gan, D. Zhang, X. Li, Microscale heat transfer enhancement using thermal boundary layer redeveloping concept, *International Journal of Heat and Mass Transfer*, 48(9), 2005, 1662-1674.
[26] H. Jonsson, B. Moshfegh, Modeling of the thermal and hydraulic performance of plate fin, strip fin, and pin fin heat sinks-influence of flow bypass, *IEEE Transactions on Components and Packaging Technologies*, 24(2), 2001, 142-149.
[27] L. Ping, D. Guo, X. Huang, Heat transfer enhancement in microchannel heat sinks with dual split-cylinder and its intelligent algorithm based fast optimization, *Applied Thermal Engineering*, 171, 2020, 115060.
[28] M.M.U. Rehman, T.A. Cheema, F. Ahmad, M. Khan, A. Abbas, Thermodynamic Assessment of Microchannel Heat Sinks with Novel Sidewall Ribs, *Journal of Thermophysics and Heat Transfer*, 34(2), 2020, 243-254.
[29] A. Faraz, T.A. Cheema, M. Mohib Ur Rehman, M. Ilyas, C.W. Park, Thermodynamic Analysis of Microchannel Heat Sink With Cylindrical Ribs and Cavities, *Journal of Heat Transfer*, 142(9), 2020, 092503.
[30] S. Assel, K.J. Tseng, Comparison of pin-fin and finned shape heat sink for power electronics in future aircraft, *Applied Thermal Engineering*, 136, 2018, 364-374.
[31] Z. Feng, I. Catton, Numerical evaluation of flow and heat transfer in plate-pin fin heat sinks with various pin cross-sections, *Numerical Heat Transfer, Part A: Applications*, 60, 2011, 107-128.
[32] A. Al-Damook, N. Kapur, J.L. Summers, H.M. Thompson, An experimental and computational investigation of thermal air flows through perforated pin heat sinks, *Applied Thermal Engineering*, 89, 2015, 365-376.
[33] K. Noda, K. Tatsumi, K. Nakabe, The Effect of Cut-fin Shape on Heat Transfer and Pressure Loss Performance, *National Heat Transfer Symposium of Japan, Japan Heat Transfer Society*, 2004.
[34] W. Al-Sallami, A. Al-Damook, H.M. Thompson, A numerical investigation of thermal airflows over strip fin heat sinks, *International Communications in Heat and Mass Transfer*, 75, 2016, 183-191.
[35] K. Ren, W. Yuan, Z. Miao, B. Yang, Influence of inlet/outlet arrangement on flow boiling of a parallel strip fin heat sink, *Applied Thermal Engineering*, 2020, 115061.
[36] A. Al-Damook, N. Kapur, J.L. Summers, H.M. Thompson, Computational design and optimisation of pin fin heat sinks with rectangular perforations, *Applied Thermal Engineering*, 105, 2016, 691-703.
[37] H.E. Ahmed, B.H. Salman, A. Sh Kherbeet, M.I. Ahmed, Optimization of thermal design of heat sinks: A review, *International Journal of Heat and Mass Transfer*, 118, 2018, 129-153.
[38] W.J. Cheng, C. Irene, M. Leng, F.J. Jinn, Optimization of pin perforation (s) induced flow dynamic for effective thermal dissipation, *International Journal of Thermal Sciences*, 152, 2020, 106308.
[39] M. Lindstedt, K. Lampio, R. Karvinen, Optimal shapes of straight fins and finned heat sinks, *Journal of Heat Transfer*, 137, 2015, 061006.
[40] J. Mahmoudi, J. Vaarno, Copper Heat Sink Design, A Practical Application of Mathematical Modelling, *Proceedings of SIMS, Sweden*, September 18-19, 2003.
[41] J. Mahmoudi, Productivity and Quality Improvement of Horizontal Casting Process at Nordic Brass, Part one, *Internal Report, Outokumpu Copper*, 2003, 1-42.
[42] J. Mahmoudi, J. Vaarno, Copper-base Heat Sink Design for Intel P4_Standard, A Practical Application of Mathematical Modeling, *Internal Report, Outokumpu Copper*, 2002, 1-27.
[43] J. Mahmoudi, J. Vaarno, Practical Application of Mathematical Modeling On the Nozzle Configuration in a Strip Casting Process; Part one: An experimental water-modeling study on the inlet nozzle jet design, *Internal Report, Outokumpu Copper*, 2001, 1-18.
[44] J. Mahmoudi, J. Vaarno, Practical Application of Mathematical Modeling On the Nozzle Configuration in a Strip Casting Process; Part two: Mathematical model, as a tool for inlet nozzle jet design, *Internal Report, Outokumpu Copper*, 2001, 1-54.
[45] J. Mahmoudi, Back ends defect (Bakändesfel) in the extrusion process at Nordic brass, *Internal Report, Outokumpu Copper*, 2002, 1-21.
[46] R. Nipple, J. Mahmoudi, Twin-Roll Strip Casting as the Next Generation Casting Machine, *Internal Report, Outokumpu Copper*, 2002, 1-46.
[47] J. Mahmoudi, Practical Application of the Mathematical Modelling on the Mould design for the next HOT -TOP trials, *Internal Report, Outokumpu Copper*, 2003, 1-33.
[48] J. Mahmoudi, Nozzle configuration in a Fikap/Vacap project, *Internal Report, Outokumpu Copper*, 2003, 1-17.
[48] J. Mahmoudi, Material Flow in Rodex process (cold extrusion), *Internal Report, Outokumpu Copper*, 2004, 1-33.
[49] J. Mahmoudi, Quality improvement in Buffalo Rolling process, *Internal Report, Outokumpu Copper*, 2004, 1-89.
[50] J. Mahmoudi, The effect of preheating and chamber temperature in material flow in extrusion process, *Internal Report, Outokumpu Copper*, 2002, 1-19.
[51] J. Mahmoudi, Rodex process for copper and Aluminum, *Internal Report, Outokumpu Copper*, 2002, 1-7.
[52] J. Vaarno, J. Mahmoudi, Planetry Rolling in Cast and Roll Process, *Internal Report, Outokumpu Copper*, 2005, 1-46.
[53] J. Mahmoudi, P. Sivesson, Mathematical modeling of fluid flow, heat transfer and solidification in a Cu-Cr strip casting process, *Internal Report, Outokumpu Copper*, 2000, 1-59.
[54] J. Mahmoudi, Some aspect of welding on copper base alloy, *Internal Report at* KTH, Stockholm, 1995.
[55] J. Mahmoudi, J. Vaarno, Heat transfer in Up-Casting process, *Internal Report, Outokumpu Copper*, 2005, 1-25.
[56] J. Mahmoudi, M. Vynnycky, P. Sivesson, H. Fredriksson, An experimental and numerical study on the modelling of fluid flow, heat transfer and solidification in a copper continuous strip casting process, *Materials Transactions*, 44, 2003, 1741-1751.
[57] J. Mahmoudi, Mathematical modelling of fluid flow, heat transfer and solidification in a strip continuous casting process, *International Journal of Cast Metals Research*, 19, 2006, 223-236.
[58] J. Mahmoudi, Modeling of flow field and heat transfer in a copper-base automotive radiator application, *International Journal of Green Energy*, 3, 2006, 25-41.
[59] M. Sadeghi, J. Mahmoudi, Experimental and theoretical studies on the effect of die temperature on the quality of the products in high-pressure die-casting process, *Advances in Materials Science and Engineering*, 2012, 2012, 434605.
[60] J. Mahmoudi, H. Nabati, An experimental study on productivity and quality improvement of horizontal continuous casting process, *International Journal of Green Energy*, 3, 2006, 185-199.
[61] M.T. Ghomi, J. Mahmoudi, A. Khalkhali, G. Liaghat, Explosive welding of unequal surface using groove method, *Transactions of the Canadian Society for Mechanical Engineering*, 36, 2012, 113-125.
[62] J. Mahmoudi, Modelling of fluid flow and heat transfer in a copper base heat sink application, In *EuroSimE 2005. Proceedings of the 6th International Conference on Thermal, Mechanial and Multi-Physics Simulation and Experiments in Micro-Electronics and Micro-Systems*, 2005.

[63] J. Mahmoudi, SIL analysis of subsea control system components based on a typical OREDA database, Quality and Reliability Engineering, 37(8), 2021, 3297-3313.
[64] J. Mahmoudi, A Four-Step Safety lntegrity Level Analysis of Numerous Subsea Control System Components, *ASCE-ASME Journal of Risk and Uncertainty in Engineering Systems, Part B: Mechanical Engineering*, 7, 2021, 031005.

ORCID iD

Jafar Mahmoudi https://orcid.org/0000-0002-4866-5912

How to cite this article: Mahmoudi J. CFD Analyses and Comparison of the Effect of Industrial Heat Sinks in Subsea Control System (SCS), *J. Appl. Comput. Mech.*, 9(1), 2023, 95–112. https://doi.org/10.22055/jacm.2022.40364.3567